# An Iterative Method for Producing Equilibrated Symmetric Three-Arm Star Polymer Melts in Molecular Dynamics

Gopinath Subramanian*

Melts of symmetric three-arm stars are generated using a novel iterative method. In this method, an equilibrated low molecular weight configuration is used to generate progressively higher molecular weights by affine scaling and equilibration. At each stage in the progression, the synthetically lowered entanglement density allows bypassing of the exponentially large relaxation times of branched polymers. The quality of equilibration was assessed by measuring the mean dimensions, distribution of dimensions, and internal length scales of the polymers. The total time required to generate the progression of equilibrated configurations was seen to scale as the Rouse time of the highest molecular weight.

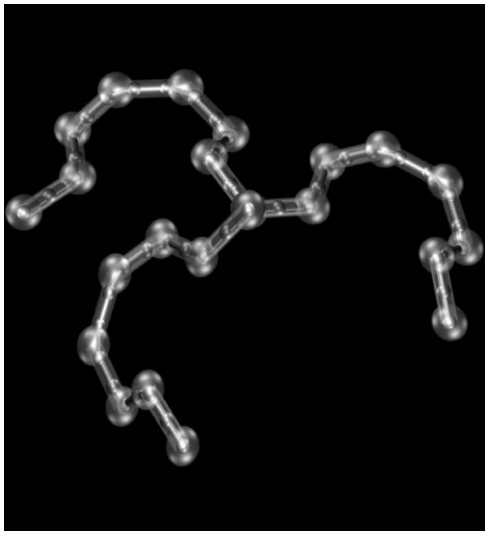

## 1 Introduction

Coarse-grained computational studies of polymers are useful in observing phenomena that are ordinarily difficult to directly observe in experiments. At the time of writing, the Kremer–Grest bead-spring model[1] is a popular coarse-grained model that has been cited over 900 times, and has been used to study the effect of cross-link density in tensile failure of glassy polymers,[2] study orientational coupling in equilibrium polymer melts,[3] examine the abilities of polymer brushes to tune surfaces,[4] and study the crossover regime between Rouse and reptation dynamics.[5] For most computational studies of polymers, a well-equilibrated initial configuration is a prerequisite. Equilibrated systems can be generated by first generating a preliminary configuration, typically using a random walk, or a self-avoiding walk. Following an energy minimization, the equations of motion are integrated. After polymers in the system have diffused, on average, a distance comparable to their size, the system is considered fully equilibrated.

This brute-force method of equilibration performs adequately for dilute solutions and low molecular weight melts, but poses serious difficulties for entangled long-chain branched polymers, such as stars, and combs. In these branched polymers, the branch point remains anchored at time scales less than the arm relaxation time. Thermal fluctuations occasionally cause an arm to retract completely, freeing the branch point to execute a hop in a random direction. A series of such hops leads to self-diffusion of the branched polymer. The arm retraction potential, in the absence of dynamic dilution, is a quadratic function of the arm molecular weight,[6,7] and therefore, the terminal relaxation time of branched polymers has an *exponential* dependence on arm molecular weight. Thus, even with modern day parallel computers, brute-force equilibration of well-entangled branched polymers can be prohibitively expensive. In order to overcome the long timescales

G. Subramanian
Scientific Computation Research Center, Rensselaer Polytechnic Institute, 110, 8th Street, Troy, New York 12180, USA
E-mail: gsub@scorec.rpi.edu




DOI: 10.1002/mats.201000062

associated with brute-force equilibration, alternative methods, similar to the polymerization process have been used.[8,9] Another set of long-standing methods includes the chain connectivity altering algorithms, that have been studied for almost two decades,[10–24] and recently generalized for application to H-shaped, pom-pom, and short-chain branched polymers by Baig et al.[25] These bridging methods all employ a plethora of complex moves that can be difficult to implement. Moreover, it may not be easy to extend these bridging algorithms to cyclic polymers, which have recently gained some attention.[26–40]

In this study, a novel method of generating equilibrated configurations of symmetric three-arm star melts is presented. While the method presented here is not necessarily faster or more efficient than the bridging methods mentioned above, it is conceptually simpler, easy to implement, not restricted to short-chain branched polymers, and can be easily generalized to potentially a wide variety of branched polymer architectures. The scaling algorithm presented in this study is a generalization of the successive molecular weight doubling (SMWD) method,[41] which has been successfully used to generate equilibrated conformations of both linear and cyclic polymers. In the original manuscript, it was shown that an equilibrated melt of cyclic polymers could be generated in approximately one Rouse time, and for reasons that are still unclear, equilibrated linear polymer melts could also be generated in a timescale on the order of one Rouse time. While it was mentioned that the SMWD algorithm could be applied to branched polymers, the timescales required for generating equilibrated branched polymers are a priori unknown. Thus, the purpose of this manuscript is the following: (1) generalize the SMWD method – i.e., show that the scaling algorithm is not restricted to a doubling of molecular weights; (2) demonstrate that although the dynamics of branched polymers can be very different from those of linear polymers, the scaling algorithm can be used to generate three-arm star melts, and that it is not restricted to short-chain branched polymers; and (3) establish the timescales associated with the scaling algorithm applied to three-arm stars. In the following sections, the model is defined and the methods for generating equilibrated melt configurations are described. The quality of equilibration is examined by measuring the mean size of polymers, the mean internal length scales of the arms, and for the first time, the distribution of arm size.

## 2 Methods

### 2.1 Model

Polymers are represented using the coarse-grained bead-spring model[1] with beads of mass $m$. Excluded volume interactions are incorporated using the Lennard-Jones potential given in Equation 1. Consecutive beads on a polymer chain are connected by the finite extensible nonlinear elastic (FENE) potential given in Equation 2.

$$U_{\mathrm{LJ}}(r) = \begin{cases} 1 + 4\varepsilon\left[(\sigma/r)^{12} - (\sigma/r)^{6}\right], & r \le R_c \\ 0, & r > R_c \end{cases} \quad (1)$$

$$U_{\mathrm{FENE}}(r) = \begin{cases} -0.5kR_o^2 \ln\left[1 - (r/R_o)^2\right], & r \le R_o \\ \infty, & r > R_o \end{cases} \quad (2)$$

In this model, the fundamental units of mass, length, time, and temperature are, respectively, $m$, $\sigma$, $\tau = \sigma(m/\varepsilon)^{1/2}$, and $T = \varepsilon/k_B$. All quantities are presented in reduced units, and are therefore dimensionless. The cutoff distance for the Lennard-Jones potential is chosen as $R_c = 2^{1/6}$, making it purely repulsive in nature. The parameters of the FENE potential were chosen to be $k = 30$ and $R_o = 1.5$. These parameters prevent excessive separation of consecutive monomers along a chain, and prevent chain crossing.[42,43] Evolution of the system is accomplished by integrating the equations of motion using a velocity Verlet algorithm[44,45] with a time step $\Delta t = 0.006$. During integration, the system temperature is rescaled to unity every 10 time steps by rescaling velocities of the beads in the system (errors associated with this thermostat are not significant for purposes of this study – see Appendix). The number density of beads in the simulation box is maintained at $\rho = 0.85$ throughout.

### 2.2 Generation of Three Arm Star Melts

In this study, the molecular weight of each arm of a star (excluding the branch point) is denoted by $N$. The molecular weight of a star polymer is therefore given by $N_{\mathrm{star}} = 3N + 1$. The number of polymers in all systems is chosen to be $N_p = 100$.

The seed configuration for the scaling algorithm is a well-equilibrated low molecular weight melt with $N = 32$. This molecular weight is low enough to ensure that the polymers are unentangled. Thus, the seed configuration is generated using the brute-force method as follows: in a simulation box of side $L$ with periodic boundary conditions, $N_p$ branch points are placed at random locations. From each branch point, three-arms, each of molecular weight $N = 32$ are grown as random walks. In order to remove overlaps between beads, the energy of the system is minimized until the total energy drops below $1 \times 10^{-30}$. The equations of motion are integrated, and the system is allowed to evolve. The center of mass of each polymer is tracked, and the seed system is considered equilibrated after the mean distance

traveled by the polymers is three times their radius of gyration.

From this equilibrated seed configuration, an iterative process is used to generate systems with a geometric progression of arm molecular weights, characterized by the common ratio $r_c$. The iterative process consists of affine scaling, replacement, and equilibration. Affine scaling and replacement are used to produce a new simulation box with polymers of arm molecular weight $N_{new} = \lfloor r_c N_{old} \rfloor$ (here, $\lfloor\ \rfloor$ denotes the floor function). Setting $r_c = 2$ reduces the scaling algorithm to the SMWD method.[41] Figure 1 shows a schematic of the affine scaling and replacement of a three-arm star with $N = 10$, $r_c = 1.1$. The coordinates of the beads, along with the simulation box are affinely scaled by a factor $k_A$. The scaling factor $k_A$ is chosen such that the new simulation box has the same number density of $\rho = 0.85$ as the old one. This affine scaling multiples the position vector of each bead in the simulation box by the scaling factor $k_A$. As a result, the angle between every arbitrary pair of vectors remains unchanged, and the length of every arbitrary vector in the simulation box is multiplied by the factor $k_A$. Thus, the affine scaling preserves the topology of the system. Each polymer is then replaced by a new polymer as follows: the normalized coordinate along the contour of an arm, including the branch point, is given by $s$. The coordinates of the end bead of an arm, and the branch point, are given by $s = 0$ and $s = 1$, respectively. The $N_{old}$ beads along the contour of every arm are replaced by $N_{new}$ beads, such that the new beads, along with the branch point, are equally spaced along the contour of the arm in the interval $s \in [0, 1]$.

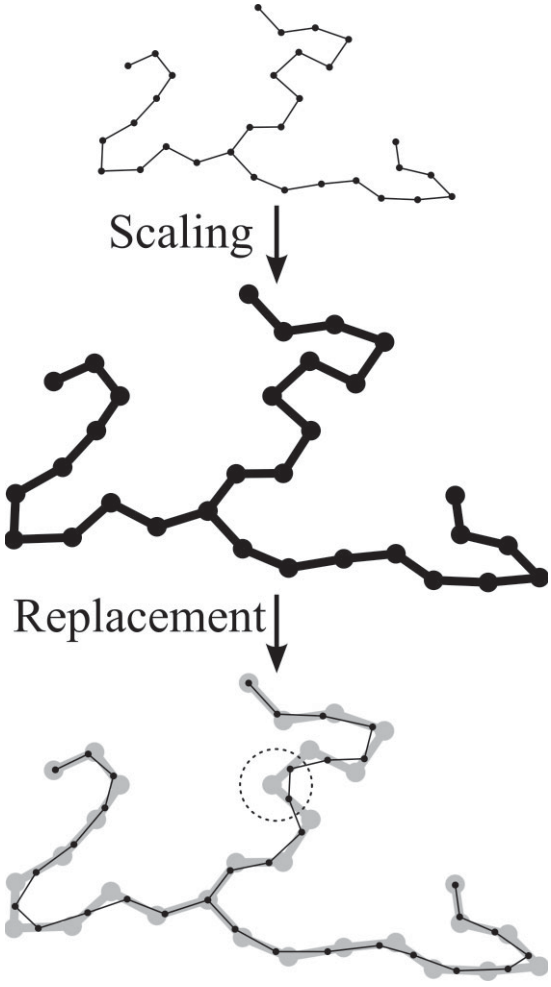


*Figure 1.* Schematic of affine scaling and replacement of a three-arm star with $N = 10$, $r_c = 1.1$. The old polymer is affinely scaled by a factor $k_A$. New beads are then placed along the contour of the scaled old polymer. The broken circle indicates a location where a local topological change might occur, when new beads are close to the mid points of the old bonds.

For the value of $r_c = 1.1$ shown in Figure 1, the contour of the new arm does not exactly follow the contour of the old arm. In particular, when two consecutive beads of the new arm are located close to the midpoints of bonds from the old arm, the deviation of the new arm from the contour of the old arm can be significant. One such configuration is indicated by a broken circle in Figure 1. If two such configurations (from two different arms, or even the same arm) are close to each other, it is possible that chain crossing might take place during replacement. However, in the equilibration of three-arm stars, or any other polymer with ends, it is not vital to prohibit chain crossing during equilibration. In fact, chain crossing has been used in the past[46] to facilitate equilibration. This is because in well-equilibrated melts, the topologies of chains that are allowed to cross are statistically indistinguishable from chains whose crossing is forbidden. It will also be seen that ignoring the effects of possible chain crossing does not affect the melt quality of three-arm stars. However, for polymers without ends, such as cyclic polymers, chain crossing will violate topological constraints, such as non-catenation and knotting. For such polymers, higher values of $r_c$ would be preferable. Other constraints that force the contour of the new chain to follow the contour of the scaled old chain can be imposed. For example, the spacing of new beads in the interval $s \in [0, 1]$ could be staggered such that the new chain exactly follows the contour of the scaled old chain. These are, however, implementation details, and thus not explored in this study.

The affine scaling and replacement preserves the random walk nature of polymers in the system, produces deformations at all length scales, and reduces the entanglement density. Thus, further equilibration becomes necessary. However, due to the lowered entanglement density, the equilibration time required is thought to be less than the terminal relaxation time. However, the actual time required to relax these deformations is somewhat unclear, as pointed out earlier.[41] In this study, each system produced by scaling and replacing the beads was allowed

to equilibrate for two Rouse times (this time of equilibration will be shown to be sufficient). At the end of this equilibration period, polymer melts with arm molecular weight $N_{new}$ were taken to be equilibrated, and used as the seed configuration for the next iteration. It must be noted here, as was pointed out by a reviewer, that since the bead-spring model is relatively soft, excess energy produced by the affine scaling and replacement can easily be absorbed. However, for hard models, such as fully atomistic, or even the bead-spring model with stiffer springs, at the very least, an intermediate energy minimization step may be required.

The Rouse time of a three-arm star was taken to be $\tau_R = \tau_e(N_{star}/N_e)^2$. This computation of the Rouse time is an overestimate, as three-arm stars adopt more compact conformations than linear polymers of equal molecular weight. The quantities relevant to calculating the Rouse time were obtained from separate simulations on linear polymers[41] as molecular weight between entanglements $N_e = 90$[a], and relaxation time of an entanglement segment $\tau_e = 10^4$.

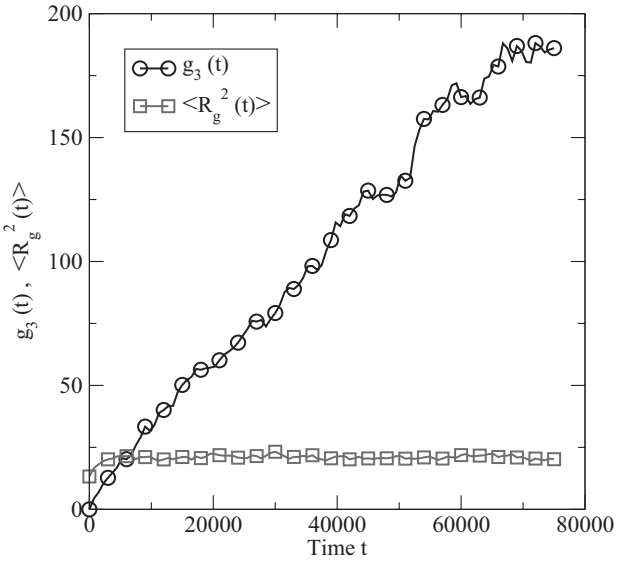


*Figure 2.* Brute-force equilibration of three-arm stars with arm molecular weight $N = 32$. At the end of the equilibration period, the stars have diffused a distance comparable to their size.

## 3 Results & Discussion

All simulations were executed using a modified version of LAMMPS.[50] Choosing the number of polymers as $N_p = 100$ ensures that the simulation box size $L$ is at least three times the average radius of gyration. The system with arm molecular weight $N = 32$ was generated using brute-force equilibration, during which time, the center of mass $\mathbf{R}_{cm}$ of all polymers was tracked. The mean square distance diffused by the center of mass of polymers in the system was computed as

$$g_3(t) = \left\langle [\mathbf{R}_{cm}(t) - \mathbf{R}_{cm}(0)]^2 \right\rangle \quad (3)$$

where the average is taken over all polymers in the system. Figure 2 shows a plot of $g_3(t)$, along with the evolution of the mean square radius of gyration $\left\langle R_g^2(t) \right\rangle$. Polymers generated using random walks are initially compressed, and quickly expand to reach their equilibrium dimensions. Since the average distance diffused by the polymers is greater than their average size, the system was considered equilibrated. This seed configuration was used to generate two different progressions of molecular weights, corresponding to $r_c = 1.1$ and $r_c = 1.5$, and the system parameters, along with the mean square radius of gyration obtained are summarized in Table 1. For all systems, the simulation box size is large enough to avoid artifacts resulting from polymers interacting with themselves across the periodic boundaries.

The size of stars generated in this study was compared with the Zimm–Stockmayer expression[51] for the contraction factor $g$. For symmetric three-arm stars, the following expression is obtained:

$$g = \frac{\left\langle R_g^2(N) \right\rangle_{star}}{\left\langle R_g^2(3N+1) \right\rangle_{linear}} = \frac{7}{9} \quad (4)$$

This expression relates the mean square radius of gyration of symmetric three-arm stars having arm molecular weight $N$ (or equivalently, polymer molecular weight $N_{star} = 3N + 1$), to the mean-square radius of gyration of linear polymers with molecular weight $N_{star}$. Rearranging, an expression for the mean square radius of gyration of stars as a function of arm molecular weight is obtained as

$$\left\langle R_g^2(N) \right\rangle_{star} = \frac{7}{18} C_\infty b^2 N \quad (5)$$

Figure 3 shows the mean square radius of gyration of three-arm stars generated in this study, along with the Zimm–Stockmayer prediction. The results are in excellent agreement for both progressions of molecular weights.

Equilibration quality of the melts was also assessed by measuring the size of the internal length scales of the arms,

[a] The molecular weight between entanglements is computed using the annealing primitive path analysis of Everaers et al.[47] Other methods of obtaining the primitive path, such as the Z-code[48] yield slightly different estimates for $N_e$[49].

*Table 1.* Summary of systems simulated. For all systems, the bead number density, and number of polymers is $\rho = 0.85$, and $N_p = 100$, respectively. The simulation box size ($L$) is at least three times the mean radius of gyration.

| $r_c = 1.1$ | | |
|---|---|---|
| $N$ | $L$ | $\langle R_g^2 \rangle$ |
| 32 | 22.51 | $21.07 \pm 0.79$ |
| 35 | 23.19 | $22.81 \pm 0.55$ |
| 38 | 23.83 | $24.63 \pm 0.46$ |
| 41 | 24.43 | $26.72 \pm 0.52$ |
| 45 | 25.20 | $29.61 \pm 0.63$ |
| 49 | 25.92 | $32.12 \pm 0.82$ |
| 53 | 26.60 | $35.11 \pm 0.72$ |
| 58 | 27.41 | $36.82 \pm 0.87$ |
| 63 | 28.17 | $43.57 \pm 0.84$ |
| 69 | 29.03 | $45.50 \pm 1.32$ |
| 75 | 29.85 | $51.11 \pm 1.23$ |
| 82 | 30.74 | $55.59 \pm 1.03$ |
| 90 | 31.71 | $60.06 \pm 0.89$ |
| 99 | 32.73 | $66.75 \pm 2.69$ |
| 108 | 33.69 | $68.62 \pm 1.22$ |
| 118 | 34.70 | $78.03 \pm 2.48$ |
| 129 | 35.74 | $83.87 \pm 1.55$ |
| 141 | 36.81 | $97.29 \pm 2.76$ |
| 155 | 37.99 | $108.11 \pm 3.98$ |
| 170 | 39.17 | $115.00 \pm 5.61$ |
| $r_c = 1.5$ | | |
| $N$ | $L$ | $\langle R_g^2 \rangle$ |
| 32 | 22.51 | $21.07 \pm 0.79$ |
| 48 | 25.74 | $31.86 \pm 0.67$ |
| 72 | 29.45 | $47.27 \pm 0.93$ |
| 108 | 33.69 | $75.52 \pm 3.21$ |
| 162 | 38.55 | $114.74 \pm 2.68$ |
| 243 | 44.12 | $174.69 \pm 3.02$ |

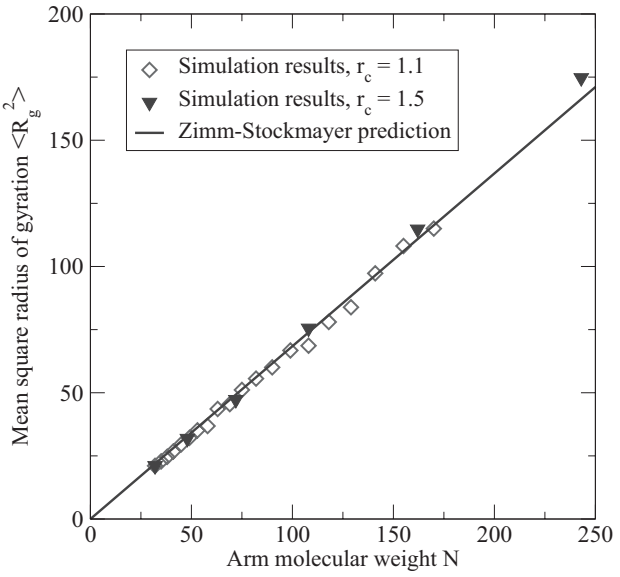


*Figure 3.* The mean-square radius of gyration of three-arm star polymers obtained in this study as a function of the arm molecular weight. Also shown is the Zimm–Stockmayer prediction.

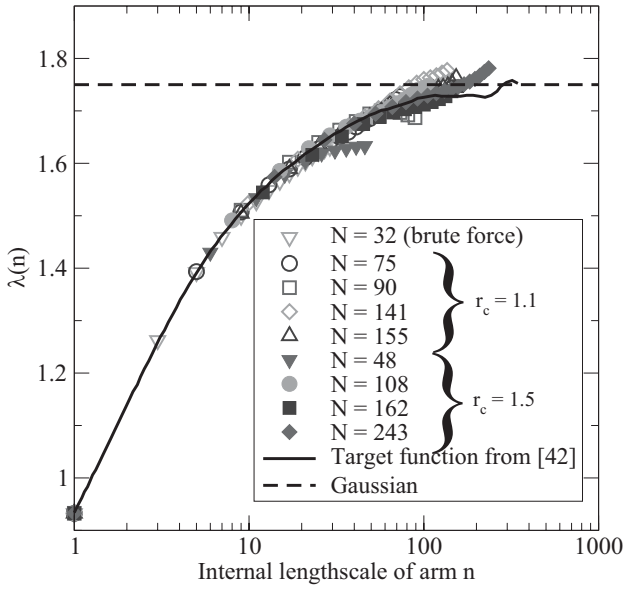


*Figure 4.* The mean square distance between beads on an arm for a few selected arm molecular weights. The solid black line is the target function from Auhl et al.,[42] and the broken black line is the Gaussian expectation.

defined as

$$\lambda(n) = \frac{\langle \mathbf{R}(n)\mathbf{R}(n) \rangle}{n} \tag{6}$$

where $\mathbf{R}(n)$ is the vector connecting two beads on an arm that are separated by $n$ bonds, and the average is taken over all possible combinations of such beads. This metric is an excellent indicator of arm configuration at all length scales, and the results are shown in Figure 4 for a few selected arm molecular weights. Also shown is the so-called target function of Auhl et al.,[42] and the Gaussian expectation. It is seen that the arms are Gaussian at all except the smallest length scales. This is because the core region of the stars is negligibly small due to the small number of arms,[52] and therefore, the arms themselves

display dimensional characteristics of linear polymers. These results indicate that the stars have attained their equilibrium dimensions at all length scales, and the structure of the polymer melt has equilibrated.

The results presented above measure the mean sizes of the polymers. Normally, this is considered sufficient to establish equilibrium. However, it is possible that the systems generated in this study, while having the same mean dimensions as at equilibrium, might have a distribution different from equilibrium. Thus, in order to further probe the quality of equilibration, the distribution of arm dimensions was measured. Since the arms behave like linear polymers, the distribution of sizes can be compared with readily available results for linear polymers. Following Koyama,[53] the normalized radius of gyration, and the normalized end-to-end distance of a linear polymer are defined as

$$r_g = \frac{R_g}{\left\langle R_g^2 \right\rangle^{1/2}} \tag{7}$$

$$r_{ee} = \frac{R_{ee}}{\left\langle R_{ee}^2 \right\rangle^{1/2}} \tag{8}$$

The probability density function (PDF) of the squared radius of gyration of linear polymers was given by Fixman,[54] and is re-written in terms of the normalized radius of gyration as

$$\Phi(r_g) = \frac{r_g}{4\pi} \int_{-\infty}^{\infty} K(s) \exp\left(-\frac{isr_g^2}{4}\right) ds \tag{9}$$

$$K(s) = \left(\frac{\sin Z}{Z}\right)^{-3/2} \tag{10}$$

$$Z = \sqrt{is} \tag{11}$$

The PDF of $r_g$ is then obtained from these expressions by direct numerical integration.

The PDF of the normalized end-to-end distance, $\Phi(r_{ee})$, is obtained from the PDF of the Gaussian end-to-end vector, $\Phi(\mathbf{R}, N)$,[55] as

$$\Phi(r_{ee}) = \sqrt{\frac{54}{\pi}} r_{ee}^2 \exp\left(-\frac{3}{2} r_{ee}^2\right) \tag{12}$$

Figure 5 shows plots of the PDFs of the normalized arm dimensions for polymers generated in this study. Here, the data for all molecular weights in a single progression are collapsed onto a master curve. The inset of these figures shows results obtained for the largest molecular weight generated in this study, viz. $N = 243$. For both progressions

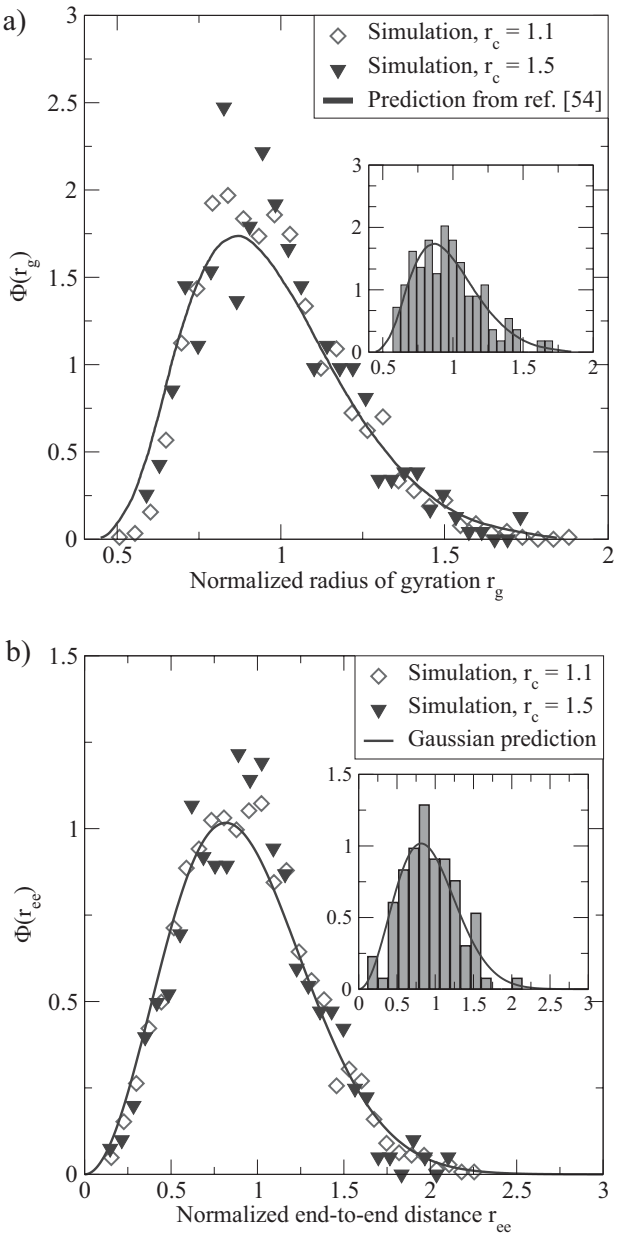


*Figure 5.* PDFs of the normalized (a) radius of gyration, $r_g$ (b) End-to-end distance, $r_{ee}$, of the individual arms of stars. The solid line shows the prediction for Gaussian linear polymers for the radius of gyration,[53,54] and the end-to-end distance (Equation 12) Inset: results obtained for $N = 243$.

of molecular weights, and for $N = 243$, the obtained distribution of arm sizes agrees well with the predicted distribution of linear polymer dimensions. There is some scatter in the data, especially for $r_c = 1.5$, but this is thought to be a result of insufficient sampling.

The total time taken to generate a progression of equilibrated configurations is simply the sum of equilibration times required after each affine scaling and replacement. The time taken to generate the seed configuration is

small, and can be neglected. Since the systems are equilibrated for a time on the order of one Rouse time, the sum of equilibration times of a geometric progression of molecular weights is on the order of the Rouse time of the largest molecular weight.[41] Thus, irrespective of the value of $r_c$, the total time taken to generate a system of molecular weight $N_{star}$ (and all the intermediate molecular weights) scales as the Rouse time of the molecular weight $N_{star}$. This is a significant savings in time when compared with brute-force methods that require a total time that scales exponentially with the molecular weight.

While the above results indicate that melts generated in this study are well-equilibrated, it is important to point out outstanding issues and questions. First, topology preservation in three arm stars is not guaranteed, but as shown above, it is not important. In situations where topology preservation is vital, the iterative method presented here will need some modifications that ensure that the new polymer follows the contour of the scaled old polymer. At the very least, the probability of chain crossing can be minimized by choosing a larger value of $r_c$.

The arms produced by affine scaling and replacement are compressed at all length scales. During the equilibration period, they expand, presumably along the contour of their respective confining tubes, to reach their equilibrium dimensions. The path by which the arms reach equilibrium, and the mechanism by which entanglements are introduced onto the arms warrant further investigation.

Lastly, the fact that a timescale on the order of one Rouse time is sufficient to generate equilibrated configurations of three very different topologies of polymers, viz. three-arm star (this work), cyclic, and linear polymers[41] is an indication that there is a unifying underlying phenomenon.

## 4 Conclusion

It was shown that symmetric three-arm star melts, whose dynamics can be very different from those of linear polymers, can be efficiently generated using the method presented in this manuscript. The timescales associated with this scaling algorithm are on the order of a Rouse time, which is a significant savings over the exponentially large relaxation timescales characteristic of branched polymer melts. While the scaling algorithm is not necessarily faster than the bridging algorithms, the method presented here is simple, and can potentially be extended with minimal modifications to polymers with other architectures, such as pom-pom, H, and comb.

## 5 Appendix: Drift of Simulation Cell

The temperature rescaling thermostat used in this study is known to generate a flying-ice cube.[56] In this phenomenon, kinetic energy associated with the internal degrees of freedom is gradually transferred to the macroscopic degrees of freedom, and the entire system eventually translates as a rigid body, with a velocity that is consistent with the prescribed temperature. The root cause of this phenomenon lies in the improper sampling of the distribution of velocities by individual beads. As system size increases, the sampling of velocities improves considerably, and the flying-ice problem becomes less significant.

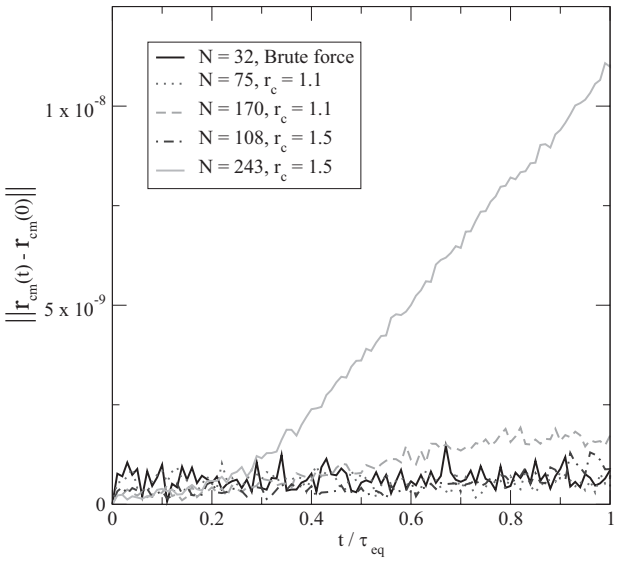


*Figure 6.* Distance traveled by the center of mass of simulation cells over the course of equilibration.

In order to determine the extent to which the flying-ice phenomenon develops in this study, the center of mass (COM) of the simulation box, denoted as $\mathbf{r}_{cm}$, was tracked. The distance traveled by the COM was computed as

$$||\mathbf{r}_{cm}(t)-\mathbf{r}_{cm}(0)|| = \sqrt{[\mathbf{r}_{cm}(t)-\mathbf{r}_{cm}(0)][\mathbf{r}_{cm}(t)-\mathbf{r}_{cm}(0)]} \quad (13)$$

Figure 6 shows a plot of distance traveled by the COM over the course of the simulations, for a few selected molecular weights. The $x$-axis is normalized by the total equilibration time, $\tau_{eq}$. The center of mass of the longest running system (with $N = 243$) considered in this study was seen to move a distance of less than $1.25 \times 10^{-8}$ reduced distance units, which is about eight orders of magnitude lower than the simulation box size. Thus, for the timescales of the simulations presented in this work, drift of the center of mass is not expected to change the results significantly.

Acknowledgements: Part of the simulations were executed on the SUR BlueGene/L at Rensselaer Polytechnic Institute, which is supported by *NSF grant 0420703*, and a gift by the IBM Corporation of a BlueGene/L computer. Thanks to *Mr. Tim*

*Wickberg* for his expert maintenance of the SCOREC computing clusters. Thanks also to *Sevan Goenezen, Nithin Mathew*, and *Ardavan Zandiatashbar* for their inputs throughout the course of the manuscript.

Received: September 7, 2010; Revised: October 7, 2010; Published online: December 1, 2010; DOI: 10.1002/mats.201000062

Keywords: branched; computer modeling; polymer melt; molecular dynamics; star polymers

[1] K. Kremer, G. S. Grest, *J. Chem. Phys.* **1990**, *92*, 5057.
[2] M. Panico, S. Narayanan, L. C. Brinson, *Modell. Simul. Mater. Sci. Eng.* **2010**, *18*, 055005
[3] J. Cao, A. E. Likhtman, *Phys. Rev. Lett.* **2010**, *104*, 207801.
[4] P. Uhlmann, H. Merlitz, J. U. Sommer, M. Stamm, *Macromol. Rapid Commun.* **2009**, *30*, 732.
[5] V. A. Harmandaris, V. G. Mavrantzas, D. N. Theodorou, M. Kröger, J. Ramrez, H. C. Öttinger, D. Vlassopoulos, *Macromolecules* **2003**, *36*, 1376.
[6] M. Doi, N. Y. Kuzuu, *J. Polym. Sci. : Polym. Lett. Ed.* **1980**, *18*, 775.
[7] S. Shanbhag, R. G. Larson, *Phys. Rev. Lett.* **2005**, *94*, 076001.
[8] J. Gao, *J. Chem. Phys.* **1995**, *102*, 1074.
[9] M. Perez, O. Lame, F. Leonforte, J. L. Barrat, *J. Chem. Phys.* **2008**, *128*, 234904.
[10] J. J. de Pablo, M. Laso, U. W. Suter, *J. Chem. Phys.* **1992**, *96*, 2395.
[11] J. I. Siepmann, D. Frenkel, *Mol. Phys. : Int. J. Int. Chem. Phys.* **1992**, *75*, 59.
[12] L. R. Dodd, T. D. Boone, D. N. Theodorou, *Mol. Phys. : Int. J. Int. Chem. Phys.* **1993**, *78*, 961.
[13] E. Leontidis, J. de Pablo, M. Laso, U. Suter, in: *Advances in Polymer Science*, Vol. 116, L. Monnerie, U. W. Suter, Eds., chapter 8, Springer, Berlin/Heidelberg 1994, pp. 283–318.
[14] P. V. K. Pant, D. N. Theodorou, *Macromolecules* **1995**, *28*, 7224.
[15] V. G. Mavrantzas, T. D. Boone, E. Zervopoulou, D. N. Theodorou, *Macromolecules* **1999**, *32*, 5072.
[16] N. C. Karayiannis, V. G. Mavrantzas, D. N. Theodorou, *Phys. Rev. Lett.* **2002**, *88*, 105503.
[17] N. C. Karayiannis, A. E. Giannousaki, V. G. Mavrantzas, D. N. Theodorou, *J. Chem. Phys.* **2002**, *117*, 5465.
[18] A. Uhlherr, S. J. Leak, N. E. Adam, P. E. Nyberg, M. Doxastakis, V. G. Mavrantzas, D. N. Theodorou, *Comput. Phys. Commun.* **2002**, *144*, 1.
[19] N. C. Karayiannis, A. E. Giannousaki, V. G. Mavrantzas, *J. Chem. Phys.* **2003**, *118*, 2451.
[20] L. D. Peristeras, I. G. Economou, D. N. Theodorou, *Macromolecules* **2005**, *38*, 386.
[21] S. W. Sides, G. S. Grest, M. J. Stevens, S. J. Plimpton, *J. Polym. Sci. Part B: Polym. Phys.* **2004**, *42*, 199.
[22] K. C. Daoulas, V. A. Harmandaris, V. G. Mavrantzas, *Macromolecules* **2005**, *38*, 5780.
[23] J. Ramos, L. D. Peristeras, D. N. Theodorou, *Macromolecules* **2007**, *40*, 9640.
[24] O. Alexiadis, K. C. Daoulas, V. G. Mavrantzas, *J. Phys. Chem. B* **2008**, *112*, 1198.
[25] C. Baig, O. Alexiadis, V. G. Mavrantzas, *Macromolecules* **2010**, *43*, 986.
[26] B. V. S. Iyer, A. K. Lele, V. A. Juvekar, *Phys. Rev. E Stat., Nonlin., Soft Matter Phys.* **2006**, *74*, 021805.
[27] B. V. S. Iyer, A. K. Lele, S. Shanbhag, *Macromolecules* **2007**, *40*, 5995.
[28] R. M. Robertson, D. E. Smith, *Macromolecules* **2007**, *40*, 3373.
[29] G. Subramanian, S. Shanbhag, *Phys. Rev. E Stat., Nonlin., Soft Matter Phys.* **2008**, *77*, 011801.
[30] G. Subramanian, S. Shanbhag, *Macromolecules* **2008**, *41*, 7239.
[31] J. Suzuki, A. Takano, T. Deguchi, Y. Matsushita, *J. Chem. Phys.* **2009**, *131*, 144902.
[32] K. Adachi, Y. Tezuka, *J. Synth. Org. Chem. Jpn.* **2009**, *67*, 1136.
[33] G. Subramanian, S. Shanbhag, *Phys. Rev. E Stat., Nonlin., Soft Matter Phys.* **2009**, *80*, 041806.
[34] T. Vettorel, A. Y. Grosberg, K. Kremer, *Phys. Biol.* **2009**, *6*, 025013.
[35] S. Nam, J. Leisen, V. Breedveld, H. W. Beckham, *Macromolecules* **2009**, *42*, 3121.
[36] Y.-B. Yang, Z.-Y. Sun, C.-L. Fu, L.-J. An, Z.-G. Wang, *J. Chem. Phys.* **2010**, *133*, 064901.
[37] G. Beaucage, A. S. Kulkarni, *Macromolecules* **2010**, *43*, 532.
[38] V. Vao-soongnern, *Comput. Mater. Sci.* **2010**, *49*, S369.
[39] S. Habuchi, N. Satoh, T. Yamamoto, Y. Tezuka, M. Vacha, *Angew. Chem.* **2010**, *122*, 1460.
[40] O. Coulembier, S. Moins, J. De Winter, P. Gerbaux, P. Leclere, R. Lazzaroni, P. Dubois, *Macromolecules* **2010**, *43*, 575.
[41] G. Subramanian, *J. Chem. Phys.* **2010**, *133*, 164902.
[42] R. Auhl, R. Everaers, G. S. Grest, K. Kremer, S. J. Plimpton, *J. Chem. Phys.* **2003**, *119*, 12718.
[43] S. K. Sukumaran, G. S. Grest, K. Kremer, R. Everaers, *J. Polym. Sci. Part B: Polym. Phys.* **2005**, *43*, 917.
[44] L. Verlet, *Phys. Rev.* **1967**, *159*, 98.
[45] L. Verlet, *Phys. Rev.* **1968**, *165*, 201.
[46] S. Shanbhag, R. G. Larson, *Macromolecules* **2006**, *39*, 2413.
[47] R. Everaers, S. K. Sukumaran, G. S. Grest, C. Svaneborg, A. Sivasubramanian, K. Kremer, *Science* **2004**, *303*, 823.
[48] M. Kröger, *Comput. Phys. Commun.* **2005**, *168*, 209.
[49] S. Shanbhag, M. Kroger, *Macromolecules* **2007**, *40*, 2897.
[50] S. Plimpton, *J. Comput. Phys.* **1995**, *117*, 1.
[51] B. H. Zimm, W. H. Stockmayer, *J. Chem. Phys.* **1949**, *17*, 1301.
[52] M. Daoud, J. P. Cotton, *J. Phys., France* **1982**, *43*, 531.
[53] R. Koyama, *J. Phys. Soc. Jpn.* **1968**, *24*, 580.
[54] M. Fixman, *J. Chem. Phys.* **1962**, *36*, 306.
[55] M. Doi, S. F. Edwards, *The Theory of Polymer Dynamics*, Oxford University Press, USA 1988.
[56] S. C. Harvey, R. K. Z. Tan, T. E. Cheatham, *J. Comput. Chem.* **1998**, *19*, 726.